PHS3350 Research project

Dirac physics of plasmons in two-dimensional electron gas

Sota Kawasaki, ID: 33857369

Supervisors: Dr. Dmitry Efimkin, Cooper Finnigan

2/2/2025

Abstract

In this report, we investigate the Dirac physics of plasmons in two-dimensional gated electron gas in a quantum mechanical manner, through the hydrodynamic and Poisson's equation. This gave a matrix which acts as a Hamiltonian, allowing us to consider a scattering problem. Furthermore, a bias current was introduced to model Fizeau drag, to determine how it affects the scattering probabilities, through calculations on Mathematica. The results incorporate the Fizeau drag in a manner which satisfies the dispersion relation, but breaks probability conservation. Some ways to improve on this have been discussed.

Acknowledgments: I would like to thank Dr. Dmitry Efimkin and Cooper Finnigan for their supervision and helping me throughout my research.

Contents

0.1 Introduction

0.1.1 Plasmon and the quantum mechanical description

Plasmons are high frequency collective density oscillations of electrons, and have been observed to occur in many types of metals and semiconductors [1]. Graphene is an excellent material for observing plasmons, due to its ability to support the propagation of long lived and tunable plasmons [2]. The mathematics behind plasmons in graphene is similar to the long wavelength behavior of waves, and will be used to explore the behaviour of plasmons in gated two-dimensional electron gas.

These plasmons can be described by the hydrodynamic equation and Poisson's equation, both of which are classical equations. Once these are linearized, however, they create a system that resembles a quantum mechanical system, which has been discussed by Finnigan et al. [3, 4]. We explored the modeling of this classical system in a quantum mechanical manner, and explored the scattering problem using this description.

0.1.2 Fizeau drag

The Michelson–Morley experiment is a commonly known experiment which was based upon the idea that light was propagating through a medium called Aether, and therefore the speed of light would change depending on the direction of "Aether winds". It is widely accepted now that there is no such thing as Aether, and the speed of light in a vacuum is constant. However this does not mean the speed of light is unaffected by the movement within a medium rather than a vacuum.

The dragging of light within the flow of water has been experimentally confirmed by Fizeau in 1851, and is commonly referred to as Fizeau drag. Furthermore, Dong et al. [2] experimentally confirmed dragging effects of surface plasmons by electron flow within graphene. This motivates us to see if we can model the dragging of plasmons by a bias current, through the previously mentioned quantum mechanical approach by applying a bias current.

0.2 Theory, method, results and analysis

0.2.1 Learning the quantum mechanical reformulation

The linearized hydrodynamic and Poisson's equation given by Finnigan et al. [3] are

$$\begin{aligned} \partial_t \rho + \nabla \cdot \vec{j} &= 0 \\ \partial_t \vec{j} &= -\frac{ne^2}{m} \nabla \phi + \frac{e}{mc}[\vec{j} \times \vec{B}], \end{aligned} \tag{1}$$

where ρ is the electron density, $\vec{j}$ is the electric current, n is the number of electrons, e is the elementary charge, m is the mass of the electron, $\vec{B}$ is an external magnetic field and ϕ is the potential. Initially we considered a system which forms a capacitor with a uniform magnetic field applied purely in the z direction, with the electrons being in x and y direction. Hence, $\phi = \frac{4\pi d}{\kappa}\rho$ and $\omega_0 = \frac{eB}{mc}$ which gives the Larmor frequency for electrons in a magnetic field of strength B. Furthermore, the plasma wave velocity is given by $u = \sqrt{\frac{4\pi n e^2 d}{m\kappa}}$. By calculating $i\partial_t$ for the currents in the x and y direction, j_x and j_y, as well as the density which was normalized to have equal dimensionality to the currents, $u\rho$, resulted in

$$i\partial_t \begin{bmatrix} j_x \\ u\rho \\ j_y \end{bmatrix} = \begin{bmatrix} 0 & u\hat{P}_x & i\omega_0 \\ u\hat{P}_x & 0 & u\hat{P}_y \\ -i\omega_0 & u\hat{P}_y & 0 \end{bmatrix} \begin{bmatrix} j_x \\ u\rho \\ j_y \end{bmatrix}, \tag{2}$$

where $\hat{P}_x$ is the momentum operator in the x direction, $-i\partial_x$, and $\hat{P}_y$ is the momentum operator in the y direction, $-i\partial_y$. We have successfully created a hermitian matrix such that $\hat{H}\psi = E\psi$, meaning this matrix acts as the Hamiltonian for our system. I then used Mathematica to determine the eigenvalues of this matrix, which was given as $\lambda = 0, \pm\sqrt{u^2p^2 + \omega_0^2}$.

0.2.2 Recovering the matrix used in the motivational paper

The next step was to recreate the matrix used in the motivational paper by Finnigan et al. [3]. This started from the same equations, equation (1) with the same assumptions for the magnetic field. We took a Fourier transform from the position and time domain to the momentum and frequency domain by taking $\partial_t \mapsto -i\omega$ and $\nabla \mapsto i\vec{q}$ where ω is the frequency and $\vec{q}$ is the wavevector, which is equivalent to the momentum by taking $\hbar = 1$. This also allows for the use of convolution, which results in the potential being $\phi = \frac{2\pi}{q\kappa}\rho$. Furthermore, the dispersion for plasma waves in the absence of a magnetic field is given as $\omega_p = \sqrt{\frac{2\pi n e^2 q}{m\kappa}}$.

As $\partial_t \mapsto -i\omega$, $\hat{E} = i\partial_t \mapsto \omega$. Hence, the reformulation of the matrix requires determining ωj^+, ωj^D, ωj^-, where $j^{\pm} = \frac{j_x \pm i j_y}{\sqrt{2}}$ and $j^D = \frac{\omega_p \rho}{q}$. This returned

$$\omega \begin{bmatrix} j^+ \\ j^D \\ j^- \end{bmatrix} = \begin{bmatrix} \omega_0 & \omega_p \frac{e^{i\phi}}{\sqrt{2}} & 0 \\ \omega_p \frac{e^{-i\phi}}{\sqrt{2}} & 0 & \omega_p \frac{e^{i\phi}}{\sqrt{2}} \\ 0 & \omega_p \frac{e^{-i\phi}}{\sqrt{2}} & -\omega_0 \end{bmatrix} \begin{bmatrix} j^+ \\ j^D \\ j^- \end{bmatrix}. \tag{3}$$

The matrix used by Finnigan et al. [3] was successfully recovered.

0.2.3 Interpreting the matrix

Now that we have the matrix, I attempted to get some meaningful information from it. The eigenvalues of this matrix was determined using Mathematica, which was given as $\lambda = 0, \pm\sqrt{\omega_0^2 + \omega_p^2}$. Let $\Omega = \sqrt{\omega_0^2 + \omega_p^2}$, which becomes the coupled frequency of the plasmons in the presence of the uniform magnetic field. By dividing the eigenvalues by ω_0 and rearranging, it can be said that $\frac{\Omega}{\omega_0} = \sqrt{\epsilon^2 + 1}$ where ϵ represents the ratio of plasma to Larmor frequency, $\frac{\omega_p}{\omega_0}$. This was plotted in figure (1).

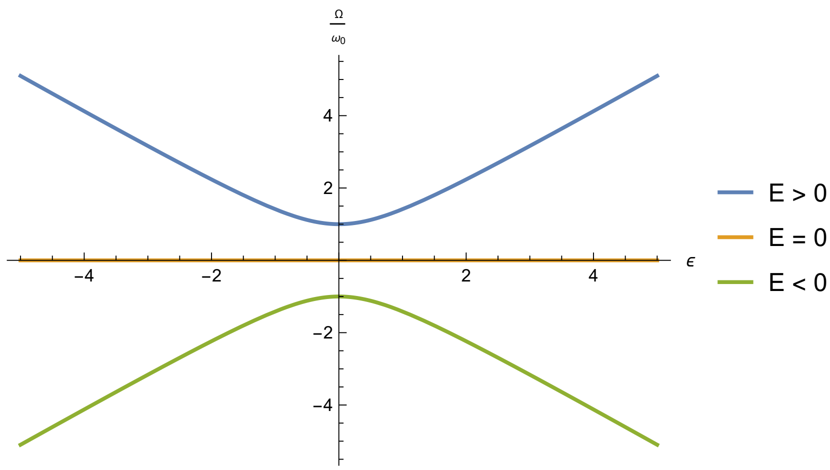

Figure 1: Plot of the ratio of coupled frequency to Larmor frequency against epsilon.

As we can see, we have a branch with 0 energy, and the positive and negative branch, both of which have a minimum frequency that is equal to the Larmor frequency. The branch of interest is the positive branch, and Mathematica returned a corresponding eigenvector of $\vec{v} = \{\frac{e^{2i\phi}\left(\omega_p^2+2\omega_0\left(\omega_0+\sqrt{\omega_0^2+\omega_p^2}\right)\right)}{\omega_p^2}, \frac{\sqrt{2}e^{i\phi}\left(\omega_0+\sqrt{\omega_0^2+\omega_p^2}\right)}{\omega_p}, 1\}$. When we look at this vector, we can see that Mathematica has normalized it in a way such that the third element is equal to 1. It is also unideal that the second term is complex, as, from our initial definition, the second term is a multiple of j^D, which is purely real. We account for these by multiplying the entire eigenvector by a constant, which returns

$$\psi = \begin{bmatrix} \frac{qe^{i\phi}}{\sqrt{2}}\left(\sqrt{\omega_0^2+\omega_p^2}+\omega_0\right) \\ q\omega_p \\ \frac{qe^{-i\phi}}{\sqrt{2}}\left(\sqrt{\omega_0^2+\omega_p^2}-\omega_0\right)\} \end{bmatrix}, \tag{4}$$

where ψ is a multiple of the eigenvector of interest. This was confirmed with Jin et al. [5], who had the same wavefunction, albeit theirs was a complex conjugate due to the way they defined their system. We would like to use this eigenvector to solve quantum mechanical problems later. This requires changing this eigenvector to a spinor, meaning it must be normalized such that $\langle\hat{\psi}|\hat{\psi}\rangle = 1$. Doing so resulted in

$$\hat{\psi} = \begin{bmatrix} \frac{e^{i\phi}}{2}(1+\frac{\omega_0}{\Omega}) \\ \frac{1}{\sqrt{2}}\frac{\omega_p}{\Omega} \\ \frac{e^{-i\phi}}{2}(1-\frac{\omega_0}{\Omega}) \end{bmatrix}, \tag{5}$$

which can be checked for normalization easily by letting $\frac{\omega_0}{\Omega} = cos\theta$ and $\frac{\omega_p}{\Omega} = sin\theta$.

0.2.4 Considering Fizeau drag

In order to add Fizeau drag to the picture, the starting equations must consider the drag as well. We will consider adding a bias current to the system. Fortunately, some of the initial work has been done by Petrov et al. [6]. Starting from the equations they worked with, but with some minor adjustments to work in our favor, we incorporated Fizeau drag into equation (1), in the form

$$\begin{gathered} \partial_t \rho + \nabla \cdot (\rho_0 \vec{u} + \vec{u}_0 \rho) = 0 \\ \partial_t \vec{j} + (\vec{u}_0 \cdot \nabla)\vec{j} = -\frac{ne^2}{m}\nabla\phi + \frac{e}{mc}[\vec{j} \times \vec{B}]. \end{gathered} \tag{6}$$

The notation is the same as what we have used before, with the additional u_0 term being the bias drift velocity, and ρ_0 being the equilibrium density, both of which we have consider to be constant. The same method was employed in order to recover a similar equation to that of equation (3). However this did not quite work due to the extra introduced term, with no clean matrix that equaled $\omega\psi$.

0.2.5 Fully incorporating the Fizeau drag

Upon close inspection, we realized the energy is no longer simply the frequency, or $i\partial_t$. Instead,

$$\hat{H}_{eff} = \omega - \vec{u}_0 \cdot \vec{q} \tag{7}$$

was used as the equation for the energy. In doing so, we successfully recovered an equation that resembles equation (3). That is,

$$(\omega - \vec{u}_0 \cdot \vec{q}) \begin{bmatrix} j^+ \\ j^D \\ j^- \end{bmatrix} = \begin{bmatrix} \omega_0 & \frac{\omega_p}{\sqrt{2}}e^{i\phi} & 0 \\ \frac{\omega_p}{\sqrt{2}}\frac{\rho_0}{\rho}e^{-i\phi} & 0 & \frac{\omega_p}{\sqrt{2}}\frac{\rho_0}{\rho}e^{i\phi} \\ 0 & \frac{\omega_p}{\sqrt{2}}e^{-i\phi} & -\omega_0 \end{bmatrix} \begin{bmatrix} j^+ \\ j^D \\ j^- \end{bmatrix}. \tag{8}$$

By considering small changes in density, we can approximate $\frac{\rho_0}{\rho} \approx 1$, resulting in a hermitian matrix that is identical to the one used in the previous works. This means the spinors we determined in equation (5) still holds, as long as we adjust for the change in expression for the Hamiltonian, given in equation (7).

0.2.6 1D Schrodinger problem with the step-like potential

Now that we have the expression for the effective Hamiltonian that incorporates the bias current, we are able to solve the scattering problem using it. As a quick refresher, we will return to the regular quantum mechanical step scattering problem, and build upon that.

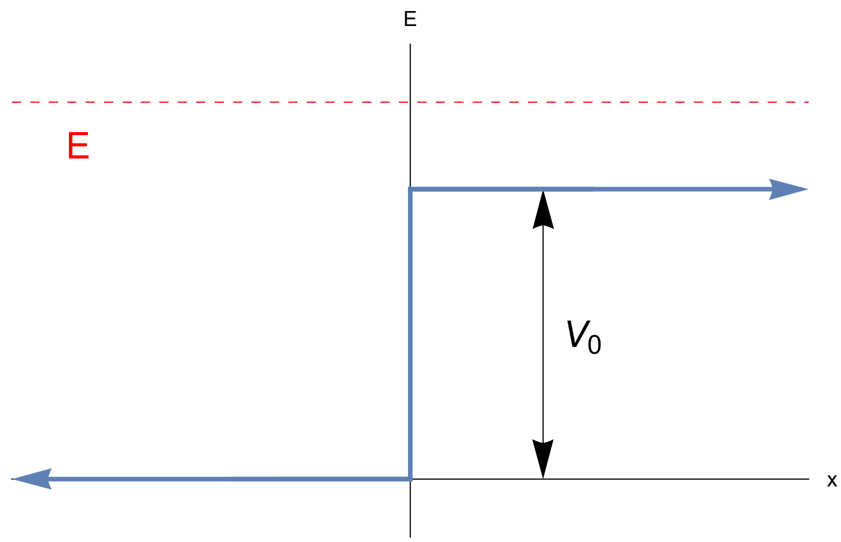

Figure 2: Quantum mechanical step scattering problem, with $E > V_0$

The simple step scattering problem is illustrated in figure (2). We will consider an incoming plane wave from the left. There will be a reflected and transmitted wave, such that

$$\begin{aligned}\Psi_L &= Ae^{iq_Lx} + Be^{-iq_Lx}\\ \Psi_R &= Ce^{iq_Rx},\end{aligned} \tag{9}$$

where A, B and C are scattering amplitudes, and q_L and q_R are the wavevectors in the left and right regions respectively. The boundary conditions that need to be satisfied are continuity and differentiability across the interface, i.e.

$$\begin{aligned}\lim_{x\to 0}\Psi_L &= \lim_{x\to 0}\Psi_R\\ \lim_{x\to 0}\partial_x\Psi_L &= \lim_{x\to 0}\partial_x\Psi_R.\end{aligned} \tag{10}$$

The two boundary conditions will return the scattering amplitudes B and C in terms of A;

$$\begin{aligned}\frac{B}{A} &= \frac{q_L - q_R}{q_L + q_R}\\ \frac{C}{A} &= \frac{2q_L}{qL + q_R}\end{aligned} \tag{11}$$

The squares of the ratios, $\left|\frac{B}{A}\right|^2$ and $\left|\frac{C}{A}\right|^2$ represent the ratios of probability densities, i.e. ratio of particles per unit length. In order to get the ratio of particles per unit time, this must be multiplied by the ratio of speeds. The speed of the wave can be determined by the momentum divided by the mass, therefore

$$\begin{aligned} R &= \frac{\frac{\hbar q_L}{m}}{\frac{\hbar q_L}{m}} \left|\frac{B}{A}\right|^2 = \left(\frac{q_L - q_R}{q_L + q_R}\right)^2 \\ T &= \frac{\frac{\hbar q_R}{m}}{\frac{\hbar q_L}{m}} \left|\frac{C}{A}\right|^2 = \frac{4 q_L q_R}{(q_L + q_R)^2}. \end{aligned} \tag{12}$$

By defining the wavevectors as $q_L = \sqrt{\frac{2mE}{\hbar^2}}$ and $q_R = \sqrt{\frac{2m(E-V_0)}{\hbar^2}}$, the reflection and transmission probabilities can be calculated in terms of the energies, and was plotted in figure (3).

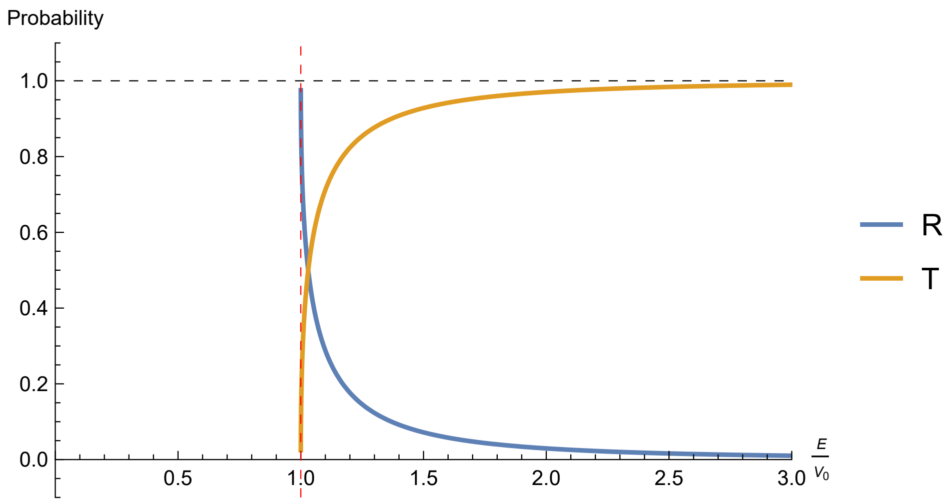

Figure 3: Plot of probability of reflection and transmission against the ratio of incoming energy to potential energy. The red dashed line shows the threshold, and the black dashed line shows the probability of 1.

0.2.7 1D plasmon scattering with the step-like magnetic field

Now that we have revisited the 1D scattering problem, it makes sense to look at the question of interest. Figure (4) shows the problem we worked with.

Figure 4: Illustration of situation of interest. The red arrow indicates the direction of flow of plasmons, and the blue arrow indicates the magnetic field. It is applied uniformly in the dark gray region, and there is no magnetic field in the light gray region.

The plasmons are excited into a region of uniform magnetic field, and are scattered off it. It is important to note that the physical system is a gated two dimensional electron gas, which means the energy is linearly proportional with the momentum under the long wavelength approximation. This problem can be seen as a one dimensional scattering problem similar to the one illustrated in figure (2), with the Larmor frequency, ω_0, being the equivalent to the barrier potential, and the incoming frequency, ω, being equivalent to the incoming energy E. The overall goal is to solve this quantum mechanical like system, and apply a bias current which acts as the Fizeau drag, to see if we can tune the reflection and transmission probabilities by altering the speed of the bias current.

Attempt 1: Directly from the Q.M. method

In the quantum mechanical scattering problem, we got an expression for the reflection and transmission probabilities in terms of the wavevectors as shown in equation (12). For my first attempt, I thought of finding the wavevectors in the problem of interest, and then substituting those into equation (12) would make sense. As $u = f\lambda$, and $f = \frac{\omega}{2\pi}$, along with $\lambda = \frac{2\pi}{q}$, we get $u = \frac{\omega}{q}$, or alternatively

$$q = \frac{\omega}{u}. \tag{13}$$

As the energy across the interface must be continuous, from equation (7),

$$uq_L - u_0 q_L = \sqrt{(uq_R)^2 + \omega_0^2} - u_0 q_R. \tag{14}$$

Solving this for q_R returns two expressions due to the relationship being quadratic. The positive branch was taken for this attempt. Upon substituting

$$q_L = \frac{\omega}{u} \tag{15}$$

we recover expressions for the reflection and transmission coefficients in terms of the velocities u and u_0, and the frequencies ω and ω_0. Let the dimensionless parameters α and γ be defined as

$$\alpha = \frac{\omega}{\omega_0}, \gamma = \frac{u_0}{u}. \tag{16}$$

Note that α is a positive value as it is a ratio of frequencies, and γ is a value ranging from -1 to 1, as it is only energetically favorable for the formation of plasmons when equation (7) is positive. These expressions for reflection and transmission probabilities were plotted in figure (5) for different values of γ. We can see that in the case of $\gamma = 0$, the plot is very similar to figure (3), with the reflection approaching 1 and transmittance approaching 0 as ω approaches ω_0, i.e. α approaches 1. However the plot does not make much sense at $\gamma > 0$, as the graph should at least continue up to $\alpha = 1$.

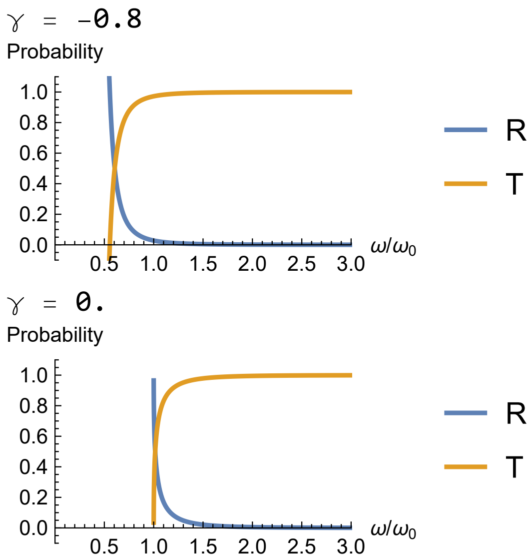

Figure 5: Plot of reflection and transmission probabilities against α for different values of γ.

Attempt 2: The other branch

To fix the discontinuity of the graph, we decided to focus on both branches of the solution in equation (14). Furthermore, we realized equation (15) was slightly wrong, with the correct expression being

$$q_L = \frac{\omega}{u - u_0}. \tag{17}$$

With these amendments, the reflection and transmission coefficients for both expressions for q_R was plotted in figure (6).

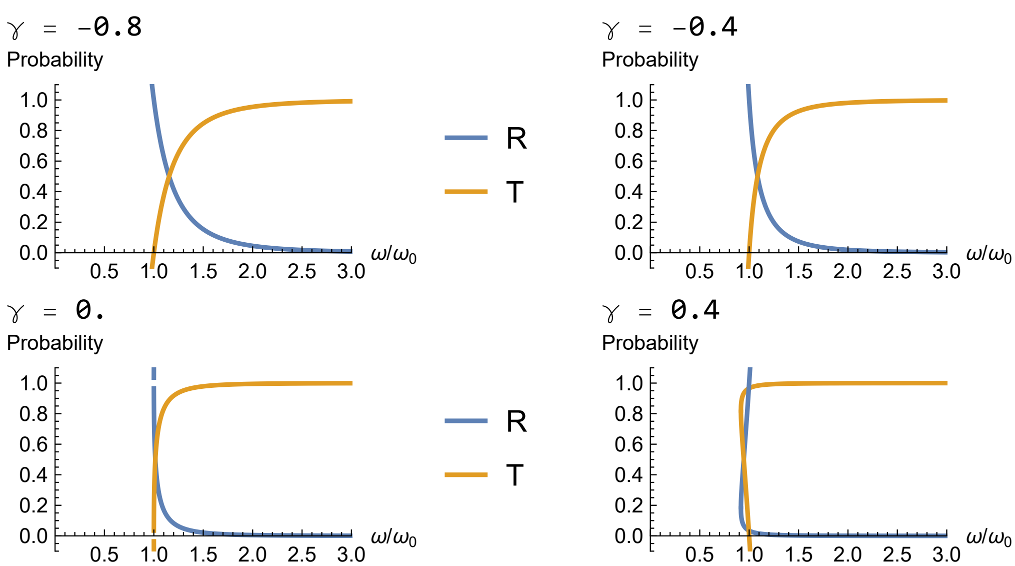

Figure 6: Plot of amended reflection and transmission probabilities against α for different values of γ.

As we can see, while the graph continues the missing part from figure (5), it does not fix the issue mentioned previously. It also returns multiple probabilities for the same frequency which does not make sense, and was therefore disregarded.

Visualizing the dispersion relation

The dispersion relation is the plot of energy against momentum, similar to that of figure (1). We revisit equation (14), and realize that the left hand side should be $u|q_L| - u_0 q_L$, as the original dispersion relation takes the magnitude of the wavevector, while the bias current considers the direction as well. Once this is plotted, we retrieve figure (7).

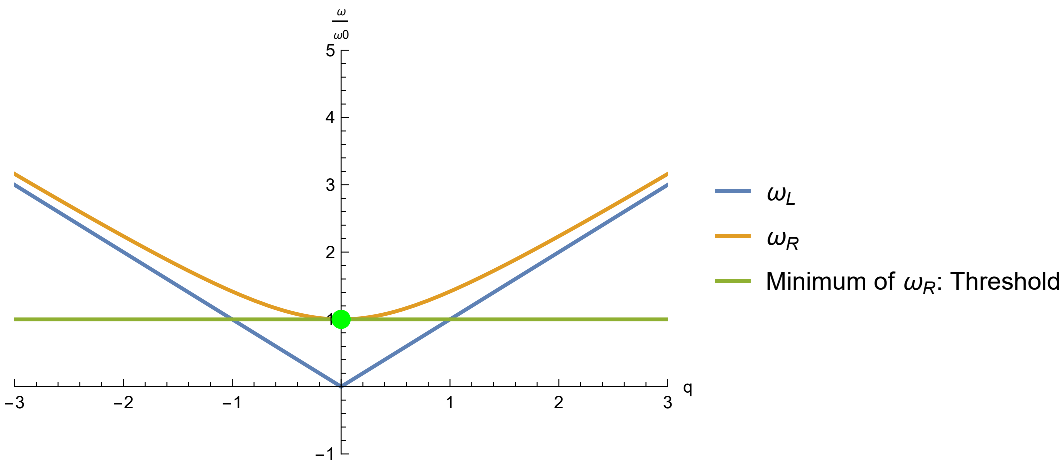

Figure 7: Dispersion relationship with $\gamma = 0$.

What is interesting, however, is when we increase γ, we get figure (8). As we can see, the minimum value of ω_R is lower than ω_0. This is symmetric with γ, meaning we require the threshold to be lower than ω_0 for all cases when $\gamma \neq 0$.

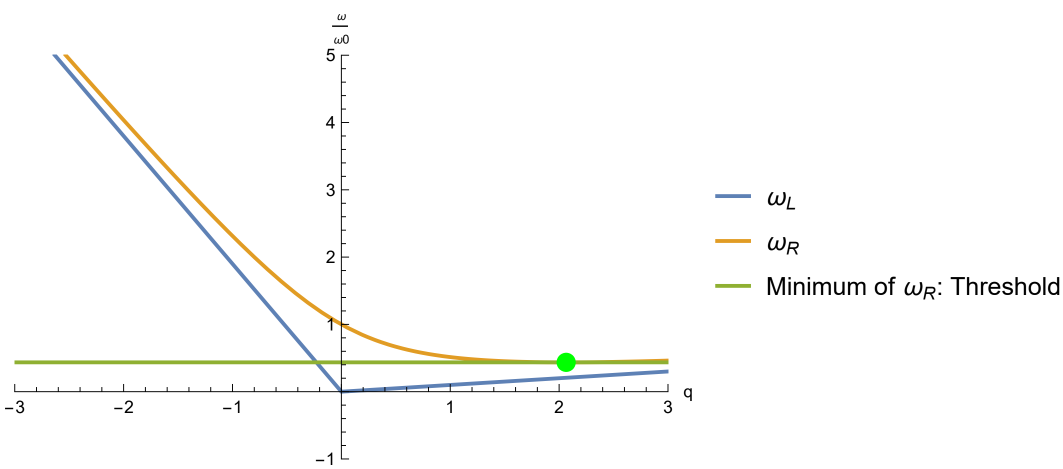

Figure 8: Dispersion relationship with $\gamma = 0.9$.

Fixing the boundary conditions

After going over the calculations, we also realised that the boundary conditions used are that for the regular scattering problem, and not for the question of interest. This means we are required to start again from equation (9). The new equations to work with are

$$\begin{aligned} \Psi_L &= A\hat{\psi}_{+q_L} e^{iq_L x} + B\hat{\psi}_{-q_L} e^{-iq_L x} \\ \Psi_R &= C\hat{\psi}_{+q_R} e^{iq_R x}, \end{aligned} \tag{18}$$

where $\hat{\psi}$ is equal to the spinors within the region, equation (5). For the left region, $\omega_0 = 0$, and $\phi = 0$ for the incoming and transmitted wave, while $\phi = \pi$ for the reflected wave, hence

$$\hat{\psi}_{+q_L} = \begin{bmatrix} \frac{1}{2} \\ \frac{1}{\sqrt{2}} \\ \frac{1}{2} \end{bmatrix}, \hat{\psi}_{-q_L} = \begin{bmatrix} -\frac{1}{2} \\ \frac{1}{\sqrt{2}} \\ -\frac{1}{2} \end{bmatrix}, \hat{\psi}_{+q_R} = \begin{bmatrix} \frac{1+\frac{\omega_0}{\Omega}}{2} \\ \frac{1}{\sqrt{2}}\frac{\omega_p}{\Omega} \\ \frac{1-\frac{\omega_0}{\Omega}}{2} \end{bmatrix}. \tag{19}$$

Due to the introduction of spinors into the equation, we can no longer use continuity and differentiability conditions. We turn to the definitions of j^+, j^D and j^- and realize $j^+ + j^- \propto j_x$ and $j^D \propto \rho$. As we are considering the one dimensional scattering problem, it makes sense to conserve the current in the x direction and the density. Hence for the boundary conditions, we took

$$\begin{aligned} \Psi_L[1] + \Psi_L[3] = \Psi_R[1] + \Psi_R[3] &\implies A - B = C \\ \Psi_L[2] = \Psi_R[2] &\implies A + B = \frac{\omega_p}{\Omega}C. \end{aligned} \tag{20}$$

Once again we have two boundary conditions, and using these we can find the scattering amplitudes B and C in terms of A;

$$\begin{aligned} \frac{B}{A} &= \frac{\omega_P - \Omega}{\omega_p + \Omega} \\ \frac{C}{A} &= \frac{2\Omega}{\omega_p + \Omega}. \end{aligned} \tag{21}$$

Attempt 3: Exploring how to define R and T

In the usual quantum mechanical scattering problems, the reflection coefficient is usually given as $\left|\frac{B}{A}\right|^2$ due to the speed of the wave being the same due to the incoming and reflected wave being in the same region. We initially started by using this, such that

$$\begin{aligned} R &= \left|\frac{\omega_P - \Omega}{\omega_p + \Omega}\right|^2 \\ T &= x\left|\frac{2\Omega}{\omega_p + \Omega}\right|^2. \end{aligned} \tag{22}$$

We aimed to find the expression for x which satisfies T for equation (22). We did this by ensuring $R + T = 1$. The results from this are plotted in figure (9).

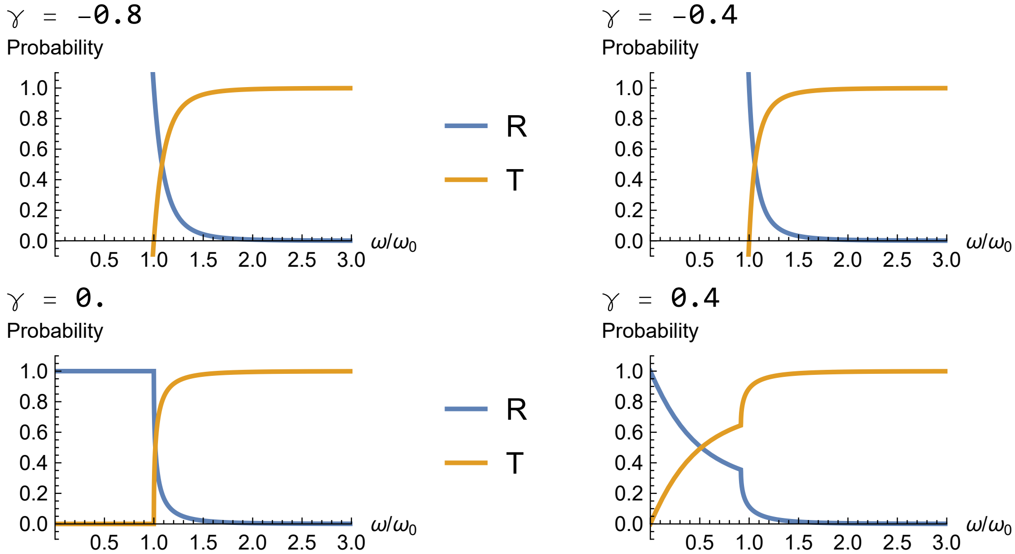

Figure 9: Plot of reflection and transmission probabilities against α for different values of γ.

These plots are very interesting, and, similar with the other plots, shows a system that makes reasonable sense in the case of $\gamma = 0$. The $\gamma > 0$ case is especially interesting, as it is saying there is a non zero probability of tunneling the moment there is even the slightest of forward current. A more concerning issue with these plots, is that the threshold is still unchanged. There is a discontinuity, or asymptote, depending on the value of γ, at $\frac{\omega}{\omega_0} = 1$, which does not agree with the results from figure (8).

Attempt 4: The best attempt achieved

The main issue currently is the fact that the threshold is unaffected by γ for the current attempts. Upon discussing this issue and working around with it, we noticed an assumption we had made which does not hold; that the speed of the incoming and reflected wave would be equal. The entire motivation of this research was the alteration of the speed of light as it moves into or against a moving medium, yet this was not taken into account. In order to properly include this into the picture, we looked at the group velocities of the plasmons. The group velocity is defined as

$$v_g = \frac{d\omega}{dq} \tag{23}$$

where v_g is the group velocity. Combining this with equation (14), we get

$$\begin{aligned} v_{gA} &= u - u_0 \\ v_{gB} &= u + u_0 \\ v_{gC} &= u\frac{\omega_p}{\Omega} - u_0 \end{aligned} \tag{24}$$

for the incoming, reflected and transmitted waves respectively. Therefore, similar reasoning to equation (12) can be used, to return

$$
\begin{aligned}
R &= \frac{u+u_0}{u-u_0}\left|\frac{\omega_p-\Omega}{\omega_p+\Omega}\right|^2 \\
T &= \frac{u\frac{\omega_p}{\Omega}-u_0}{u-u_0}\left|\frac{2\Omega}{\omega_p+\Omega}\right|^2 .
\end{aligned} \tag{25}
$$

This result was then plotted on figure (10).

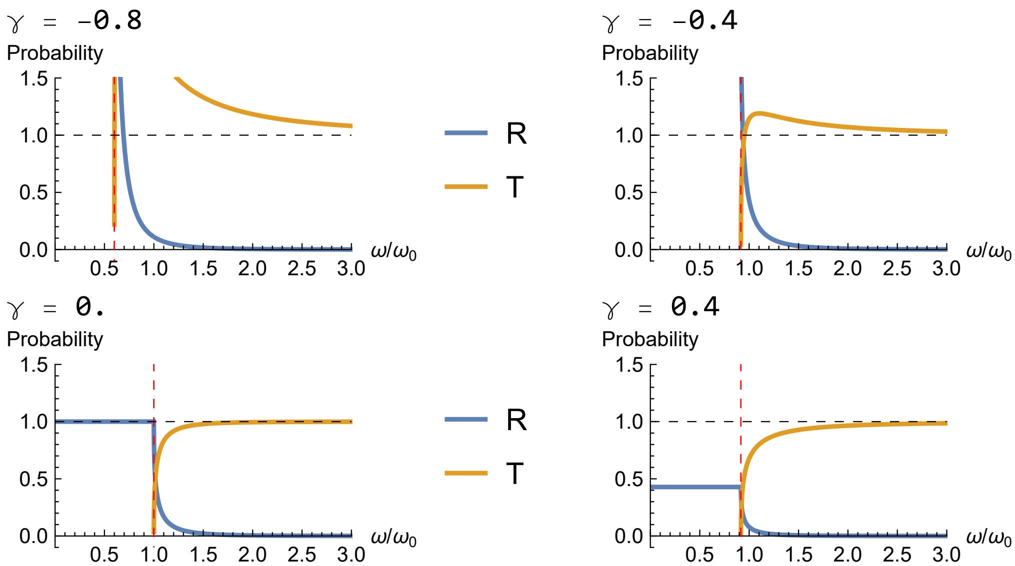

Figure 10: Plot of reflection and transmission probabilities against α for different values of γ. The red dashed line shows the threshold determined in figure (7), and the black dashed line indicates a probability of 1. Note that the vertical axis is scaled more than the other graphs to show the full picture.

Clearly, we are breaking probability conservation, as we have both R and T exceeding 1 in some cases, and even if they do not exceed 1, they do not add up to 1. The only case which makes physical sense is when $\gamma = 0$, which was always the case that worked. However, these results are not useless. We can see that in all the cases, the transmission probability approaches 0 and the reflection probability asymptotes at the red dashed line, which indicates the threshold at the given value of γ, which is an improvement from the past plots.

0.3 Discussion

Due to time constraints, figure (10) was the final attempt that could be achieved. Overall this was achieved by solving equation (25) with q_R from the positive branch of equation (14), along with equation (17) and equation (16). While some improvements or alterations to this have been discussed, none have been achieved yet. Some potential ideas for future research have been listed.

0.3.1 Checking over the calculations

While nobody involved in the research has noticed any mathematical mistakes, there is a possibility that some small point was overlooked or not done correctly. We discussed some mathematical justifications for the steps done, though.

What is being conserved?

The total density that is being conserved can be considered as $\Sigma\bar{\psi}\psi = J^2 + u^2\rho^2$. With small manipulation, it can be said that

$$\frac{\Sigma\bar{\psi}\psi}{2\rho_0} = \frac{(m\rho_0)u^2}{2} + \frac{(e\rho)^2}{2C} \approx \frac{LI^2}{2} + \frac{q^2}{2C}. \tag{26}$$

We have divided the sum of conserved properties by $2\rho_0$, which is a constant. This results in an equation that is similar to the total energy in a capacitor inductor system. This means that we have attempted to conserve the equivalent energy of a capacitor and the energy of an inductor individually. If we try to conserve the total energy by adding the elements in the spinors, we will only have one boundary condition and therefore cannot solve for the scattering problem. This means we would require one more boundary condition to continue with this idea.

Normalize by dividing by the sum

One quick fix to ensure the probability is conserved is by dividing R and T by the sum of them, ensuring they add up to 1. This was attempted and plotted in figure (11). As we can see, this does fix the issue of $R + T \neq 1$, as well as still accounting for the altered threshold. However, from figure (10), we can see that R+T does not add up to a constant, meaning at different values of $\frac{\omega}{\omega_0}$, R and T are being multiplied by different values. This does not have any mathematical justification, and therefore was not considered a proper scientific method, and was disregarded.

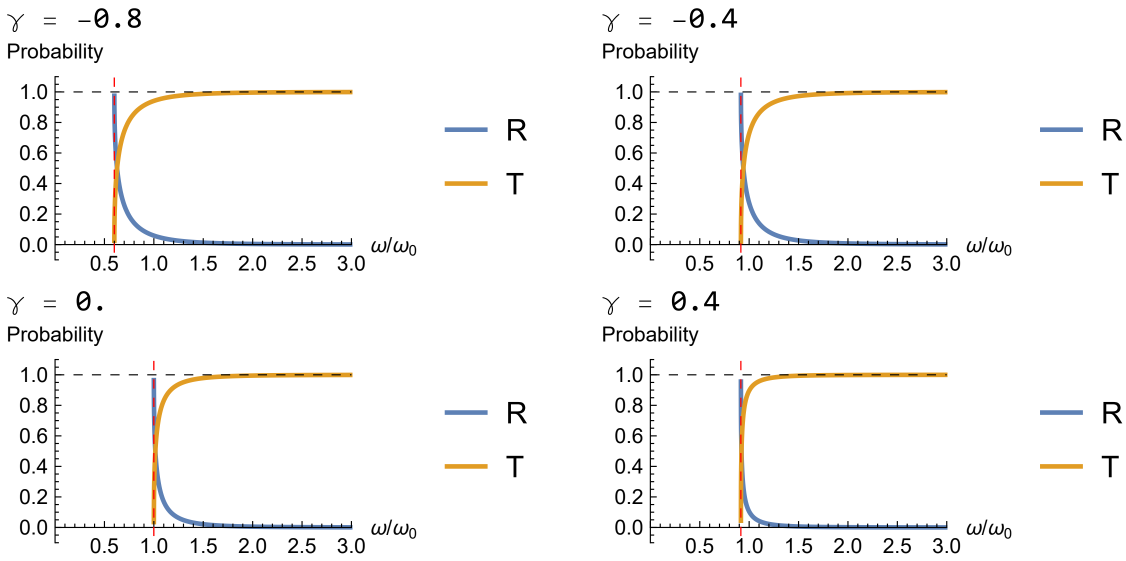

Figure 11: Plot of reflection and transmission probabilities against α for different values of γ. The red dashed line shows the threshold determined in figure (1), and the black dashed line indicates a probability of 1.

0.3.2 Considering alternative methods

The main point of our research was to solve the quantum mechanical like problem, and therefore using an alternative approach for the reformulation is unideal. However, we can consider a different approach for the one dimensional scattering problem. One known potential which has an analytical solution is the Rosen-morse potential. While the exact mathematics was not explored due to the lack of time, a potential similar to figure (12) might work great for this question.

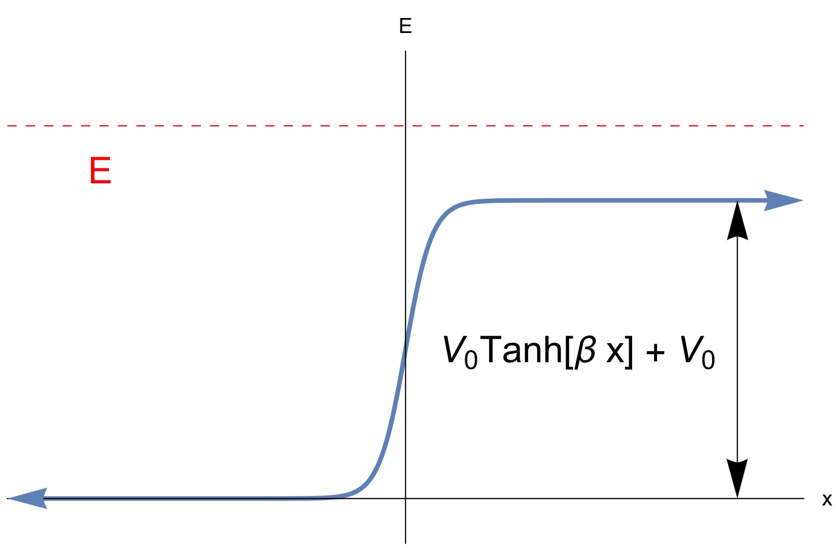

Figure 12: Scattering with a Rosen morse potential.

By taking the limit as β approaches infinity for the plot in figure (12), this would approach a step scattering problem. As the potential is continuous, this approach would not require any boundary conditions, removing the issue of being unsure with what boundary conditions to use.

0.4 Conclusion

Throughout the process of this research project, we have successfully managed to model the classical system in a quantum mechanical manner, and solved the scattering problem. It can be seen that the plots resulted are very similar to a regular quantum mechanical scattering problem, with the reflection reaching 1 and the transmittance approaching 0 as the incoming energy approaches the threshold. However as it can be seen from figure (10), the introduction of the bias current results in the destruction of conservation of probability. That being said, it does exhibit some important traits, such as the reflection assymptoting and the transmittance reaching 0 at the threshold, and the reflection approaching 0 as the incoming frequency becomes large.

Bibliography

[1] A. N. Grigorenko, M. Polini, and K. S. Novoselov. Graphene plasmonics. *Nature Photonics*, 6(11):749–758, November 2012.

[2] Y. Dong, L. Xiong, I. Y. Phinney, Z. Sun, R. Jing, A. S. McLeod, S. Zhang, S. Liu, F. L. Ruta, H. Gao, Z. Dong, R. Pan, J. H. Edgar, P. Jarillo-Herrero, L. S. Levitov, A. J. Millis, M. M. Fogler, D. A. Bandurin, and D. N. Basov. Fizeau drag in graphene plasmonics. *Nature*, 594(7864):513–516, June 2021.

[3] Cooper Finnigan, Mehdi Kargarian, and Dmitry K. Efimkin. Equatorial magnetoplasma waves. *Physical Review B*, 105(20), May 2022.

[4] Cooper Finnigan and Dmitry K. Efimkin. Giant resonant skew scattering of plasma waves in a two-dimensional electron gas, 2024.

[5] Dafei Jin, Ling Lu, Zhong Wang, Chen Fang, John D. Joannopoulos, Marin Soljačić, Liang Fu, and Nicholas X. Fang. Topological magnetoplasmon. *Nature Communications*, 7(1), November 2016.

[6] Aleksandr S. Petrov and Dmitry Svintsov. Thresholdless excitation of edge plasmons by transverse current. *Physical Review B*, 102(12), September 2020.